Am J Physiol Heart Circ Physiol 294: H433–H440, 2008.
First published November 16, 2007; doi:10.1152/ajpheart.01165.2007.

Cardiac alternans in embryonic mouse ventricles

Carlos de Diego,* Fuhua Chen,* Lai-Hua Xie, Amish S. Dave, Mya Thu, Christine Rongey, James N. Weiss, and Miguel Valderrábano

Cardiovascular Research Laboratory, Departments of Medicine (Cardiology) and Pediatrics, David Geffen School of Medicine, University of California-Los Angeles, Los Angeles, California

Submitted 8 October 2007; accepted in final form 7 November 2007

de Diego C, Chen F, Xie LH, Dave AS, Thu M, Rongey C, Weiss JN, Valderrábano M. Cardiac alternans in embryonic mouse ventricles. *Am J Physiol Heart Circ Physiol* 294: H433–H440, 2008. First published November 16, 2007; doi:10.1152/ajpheart.01165.2007.—T-wave alternans, an important arrhythmogenic factor, has recently been described in human fetuses. Here we sought to determine whether alternans can be induced in the embryonic mouse hearts, despite its underdeveloped sarcoplasmic reticulum (SR) and, if so, to analyze the response to pharmacological and autonomic interventions. Immunohistochemistry confirmed minimal sarcoplasmic-endoplasmic reticulum Ca-ATPase 2a expression in embryonic mouse hearts at embryonic day (E) 10.5 to E12.5, compared with neonatal or adult mouse hearts. We optically mapped voltage and/or intracellular Ca (Ca_i) in 99 embryonic mouse hearts (dual mapping in 64 hearts) at these ages. Under control conditions, ventricular action potential duration (APD) and Ca_i transient alternans occurred during rapid pacing at an average cycle length of 212 ± 34 ms in 57% (n = 15/26) of E10.5-E12.5 hearts. Maximum APD restitution slope was steeper in hearts developing alternans than those that did not (2.2 ± 0.6 vs. 0.8 ± 0.4; $P < 0.001$). Disabling SR Ca_i cycling with thapsigargin plus ryanodine did not significantly reduce alternans incidence (44%, n = 8/18, P = 0.5), whereas isoproterenol (n = 14) increased the incidence to 100% ($P < 0.05$), coincident with steepening APD restitution slope. Verapamil abolished Ca_i transients (n = 9). Thapsigargin plus ryanodine had no major effects on Ca_i-transient amplitude or its half time of recovery in E10.5 hearts, but significantly depressed Ca_i-transient amplitude (by 47 ± 8%) and prolonged its half time of recovery (by 18 ± 3%) in E11.5 and older hearts. Embryonic mouse ventricles can develop cardiac alternans, which generally is well correlated with APD restitution slope and does not depend on fully functional SR Ca_i cycling.

calcium cycling; cardiac development

T-WAVE ALTERNANS HAS BEEN recognized as an important risk marker of sudden cardiac death (18, 22). At the cellular level, both action potential duration (APD) and intracellular Ca (Ca_i) transient amplitude typically alternate together due to their bidirectional coupling (i.e., APD directly affects Ca_i transient amplitude, and the Ca_i transient amplitude directly affects APD via Ca-sensitive currents, such as the L-type Ca current and electrogenic Na/Ca exchange) (32). Factors promoting cardiac alternans include steep APD restitution slope (9, 17) and sarcoplasmic reticulum (SR) Ca_i cycling dynamics (5, 6). In adult ventricular muscle, current evidence (5, 11, 19) suggests that, as heart rate increases, the Ca_i cycling instability develops first and typically causes the onset of alternans (5, 8, 11, 19), although the interaction with APD restitution properties is important in influencing the onset, amplitude, and pattern (25), especially as the heart rate increases further. In embryonic heart, however, the Ca_i transient is predominantly generated by transsarcolemmal Ca entry through the voltage-dependent Ca channels rather than SR Ca release (2, 13, 15). How quickly the SR matures and contributes to excitation-contraction coupling among different tissues in the embryonic heart remains controversial (12, 14, 31). Nevertheless, a recent human fetal study reported that T-wave alternans could be detected in utero and was related to ventricular arrhythmias (33). To investigate prenatal alternans further, we studied embryonic mouse hearts using optical mapping to *1*) determine whether APD and Ca_i transient alternans can be induced by rapid pacing; *2*) address its relationship to the development of SR Ca_i cycling function; and *3*) evaluate its response to pharmacological interventions and autonomic factors during embryonic development, since we previously reported that both β-adrenergic and muscarinic receptors are present and functional in the embryonic mouse hearts at embryonic day (E) 10.5 or older (4).

METHODS

Dissection of embryonic mouse hearts. This study conformed to the Guide for the Care and Use of Laboratory Animals, published by the National Institutes of Health (NIH Publication No. 85–23, Revised 1996), and protocols were approved by the Chancellor's Animal Research Committee of the University of California at Los Angeles. Pregnant mice with different embryonic age groups were first sedated by inhalation of isoflurane and then killed by cervical dislocation (21). The uterus was dissected, and whole embryos were exposed. Embryonic mouse hearts were then isolated under a dissecting microscope, while bathed in modified oxygenated Tyrode solution containing (mmol/l) 136 NaCl, 5.4 KCl, 0.1 $CaCl_2$, 0.33 NaH_2PO_4, 1 $MgCl_2$, 10 HEPES, and 10 glucose, pH 7.3. The same solution was used as the standard bath solution in experiments with 1.8 mmol/l $CaCl_2$.

Stimulation protocol. Unipolar stimuli were delivered at the ventricle at 20- to 40-V output using silver chloride electrodes and a Grass stimulator triggered by computer-controlled pacing sequences. Specimens were paced at 2 Hz, followed by a rapid pacing protocol, initially at 340-ms cycle length (CL), decremented by 20 ms every eight beats until reaching 140-ms CL, and then incremented by 20 ms every eight beats back to 340 ms.

Optical mapping system. Isolated E10.5–E12.5 embryonic mouse hearts (total n = 99; E10.5 hearts, n = 27; E11.5 hearts, n = 32; and E12.5 hearts, n = 40) were incubated with the Ca indicator Rhod-2-acetoxymethyl ester (5 μmol/l) and pluronic F-127 (0.1%) dissolved in dimethyl sulfoxide for 40 min, as previously described (30). In 64 embryonic mouse hearts, Ca dye staining was followed by an additional 5-min incubation with the voltage indicator RH-237 (5 μmol/l). The embryonic mouse hearts were then washed in Tyrode solution before transfer to the experimental chamber on a modified inverted microscope and superfused at 37°C with Tyrode solution. Green light

* C. de Diego and F. Chen contributed equally to this work.

Address for reprint requests and other correspondence: J. N. Weiss, Division of Cardiology, 3645 MRL Bldg., David Geffen School of Medicine at UCLA, Los Angeles, CA 90095 (e-mail: jweiss@mednet.ucla.edu).

The costs of publication of this article were defrayed in part by the payment of page charges. The article must therefore be hereby marked "*advertisement*" in accordance with 18 U.S.C. Section 1734 solely to indicate this fact.

(520 ± 20 nm) from a high-intensity, light-emitting diode (Luxeon, Calgary, Canada) delivered via the microscope lens was focused on the heart; fluorescence was collected through the lens and split with a 630-nm dichroic mirror, such that passed light (>630 nm) was filtered through a 710-nm long-pass filter (voltage signal) and reflected light (<630 nm) was filtered through a 585 ± 20 nm filter (Ca signal). All filters were obtained from Chroma (Rockingham, VT). Ca and voltage signals were simultaneously recorded with two electron-multiplier charge-coupled device cameras operating at 200–500 frames/s (Photometrics Cascade 128+, Tucson, AZ) with a spatial resolution of 128 × 128 pixels ($n = 64$ specimens). In some specimens, Ca alone was recorded using a different charge-coupled device camera (model LCL 811K, Watek America, Las Vegas, NV) at 30 frames/s.

Specimens were optically mapped under control conditions and after the addition of one or more of following drugs to the Tyrode solution: *1*) β-adrenergic agonist isoproterenol (Iso; 1 μmol/l, $n = 23$); *2*) the muscarinic receptor agonist carbachol (CCh; 10 μmol/l, $n = 6$); *3* and *4*) ryanodine and thapsigargin (Ry: 10 μmol/l; and Tg: 200 nmol/l; $n = 39$); and *5*) verapamil (20 μmol/l, $n = 9$). 2,3-Butanedione monoxime (10 mmol/l) was used as an electromechanical uncoupler to reduce motion artifact. Experiments were conducted at 37°C.

Data analysis. Data were analyzed with custom software. After spatiotemporal filtering, APD at 80% repolarization (APD_{80}) was measured as the time interval during which fluorescence exceeded 20% of the baseline diastolic value at each pixel. Ca_i transient amplitude was measured as the increase in fluorescence (arbitrary units) from onset to peak (arbitrary units). To assess the effects of short-acting agents (Iso, CCh, and verapamil) on Ca_i transient amplitude, we compared pre- and postdrug Ca_i transient amplitudes directly. However, because treatment with Tg and/or Ry required 30-min incubation (during which dye bleaching and other factors made comparison to the predrug Ca_i transient amplitude unreliable), we assessed the effects of Tg and Ry on Ca_i transient amplitude by dividing each batch of embryonic hearts on a given day into a control group and treated group. Using identical loading and imaging conditions, Ca_i transient amplitudes (as the change in absolute fluorescence units) were measured after 30 min in the control and treated groups and compared. The half time of Ca_i removal was measured from the peak of the Ca_i transient to 50% of the return to baseline. APD alternans and Ca_i alternans were quantified by subtracting APD [change in APD (ΔAPD)] and Ca_i transient amplitude (ΔCa_i), respectively, of consecutive beats. We considered APD and Ca_i alternans to be present if alternation persisted until the pacing protocol was completed using thresholds of $\Delta APD > 10$ ms and $\Delta Ca_i > 10\%$ between successive beats. Onset of alternans was defined as pacing CL at which alternans was first detected during the decreasing CL phase (340–140 ms) of the pacing protocol. Offset of alternans was defined as the pacing CL at which alternans was not longer detectable during the increasing CL phase (140–340 ms) of the pacing protocol. Spatial maps of ΔCa_i and ΔAPD were generated for two consecutive beats using shades of red for positive ΔAPD (i.e., short-long APD) or ΔCa_i (i.e., small-large Ca amplitude), and shades of green for negative ΔAPD (i.e., long-short APD) or ΔCa_i (i.e., large-small Ca amplitude). APD restitution curves were generated by plotting APD against diastolic intervals (DI) and fitting to a single exponential using Origin (Microcal) software. The maximum APD restitution slope was obtained from the first derivative of the monoexponential curve at the shortest DI that elicited 1:1 capture.

Immunofluorescence labeling. As previously reported (4), immunostaining of sarcoplasmic-endoplasmic reticulum Ca ATPase 2a (SERCA2a) was performed on paraffin-embedded tissue sections. Briefly, isolated hearts of different age groups (embryonic mouse ventricles at E10.5–E12.5; 1-day-old neonate mouse ventricles, and 3-mo-old adult mouse ventricles) were fixed with 4% formalin, dehydrated with graded alcohol, cleared in xylene, and embedded in paraffin wax. A total of four heart sections were analyzed for each group. Transmural sections of 3–5 μm were cut both perpendicular and parallel to the epicardium from a paraffin-embedded tissue and mounted onto slides. Slides were incubated with protein block solution, and then sections were incubated with primary antibody of SERCA2a (Affinity BioReagents, Golden, CO) for 1 h and with secondary antibodies for 45 min. Cell membrane was stained using wheat germ agglutinin coupled to fluorescein isothiocyanate (Vector Laboratories, Burlingame, CA) for 45 min. Finally, the section slides were stained with 4,6-diamidino-2-phenylindole (Sigma, St. Louis, MO; nuclear staining) for 2 min, washed two times in normal Tyrode solution, and then mounted on slides. Control experiments were performed by exposing the tissue sections to the secondary antibody alone. All slides were viewed on an epifluorescence microscope and digitally photographed for analysis. To estimate quantitative differences in SERCA2a expression at different ages, the ratio of SERCA2a fluorescence intensity to nuclear fluorescence intensity and the ratio of SERCA2a fluorescence intensity to membrane fluorescence intensity were measured in each section, averaged, and compared between hearts at different ages.

Statistics. Data are shown as means ± SD. Statistical tests included χ^2 test and Student's *T*-test. *P* values <0.05 were considered significant.

RESULTS

SR function in developing embryonic mouse hearts. It has been suggested that the SR is neither fully developed (2, 13, 15) nor functionally well coupled to the L-type Ca current during embryonic development (31). We performed immunohistochemical and pharmacological studies to assess the status of SR Ca cycling in developing embryonic mouse hearts. Immunostaining for SERCA2a showed that the cardiac SR Ca uptake pump was detectable as early as E10.5–E12.5, but at much lower intensity relative to nuclear and membrane staining than in neonatal or adult hearts (Fig. 1). Using the identical labeling protocols and imaging settings, the ratios of SERCA2a fluorescence intensity to either nuclear fluorescence intensity or membrane fluorescence intensity in the same cardiac section were measured. Figure 1*B* shows that both ratios were much lower in E10.5 and E12.5 embryonic hearts than neonatal or adult hearts.

To assess whether SR Ca cycling is functional at these embryonic stages, we investigated the effects of blocking SR function with the SERCA2a inhibitor Tg (200 μmol/l) plus the SR Ca release channel inhibitor Ry (10 μmol/l). We also studied the effects of β-adrenergic activation with Iso (10 μmol/l) and L-type Ca channel inhibition with verapamil (20 μmol/l).

At E10.5, the combination of Tg+Ry only mildly decreased Ca_i transient amplitude to 90 ± 6% of the control value ($P < 0.01$) and did not significantly affect the half time for Ca_i removal (Fig. 1, *C* and *D*). Iso increased Ca_i transient amplitude (to 115 ± 5%, $P < 0.05$), as expected from augmenting the L-type Ca current, but did not significantly shorten the half time of Ca_i removal.

In contrast, at E11.5, Tg+Ry significantly depressed Ca_i transient amplitude to 53 ± 8% (Fig. 1*C*) and prolonged the half time for Ca_i removal (145 ± 28 vs. 119 ± 24 ms for control, $P < 0.01$) (Fig. 1*D*). Iso increased the Ca transient amplitude (to 113 ± 7%, $P < 0.01$) (Fig. 1*C*) and also shortened the half-time for Ca_i removal (to 106 ± 9 ms, $P < 0.05$) (Fig. 1*D*), similar to adult hearts in which Iso shortens the half time of Ca_i removal due to enhanced SERCA2a activity

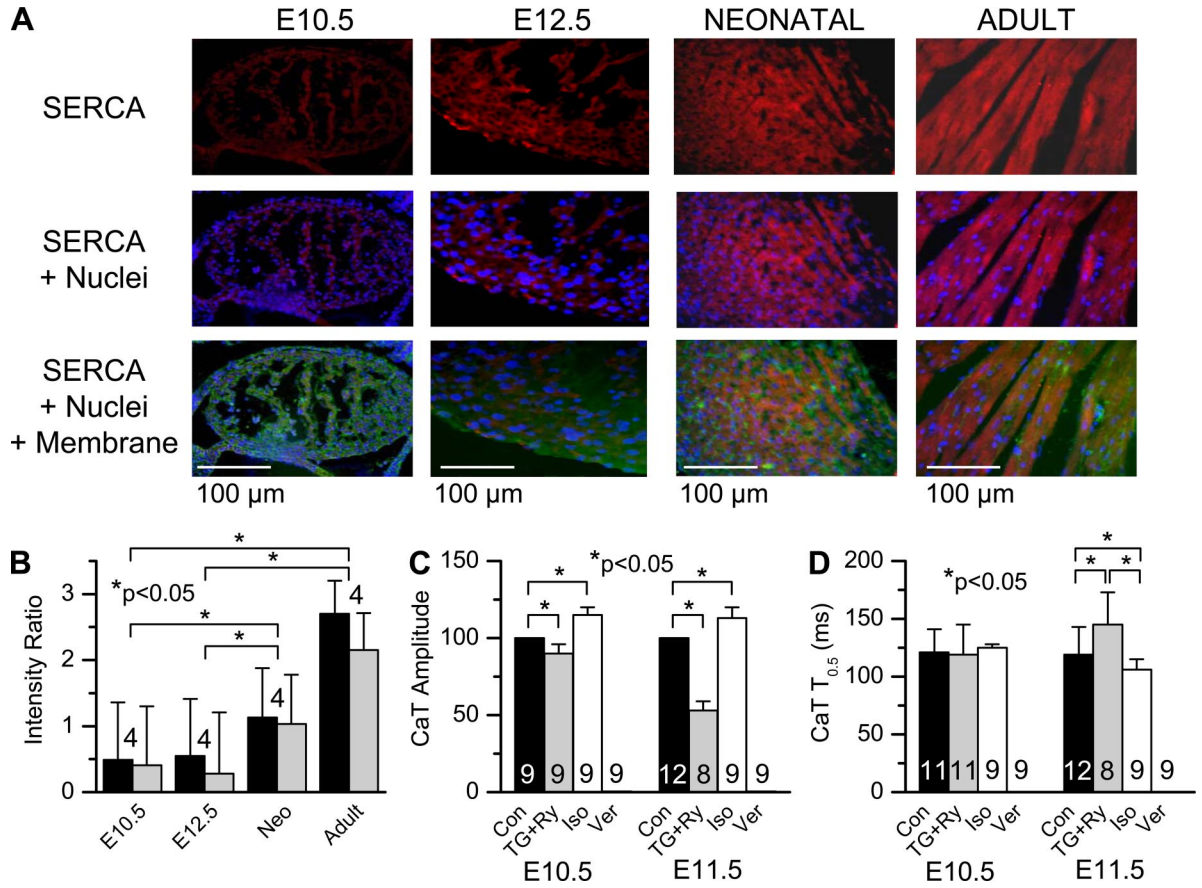

Fig. 1. Sarcoplasmic reticulum (SR) features in embryonic mouse hearts. *A*: immunostaining of sarcoplasmic-endoplasmic reticulum Ca ATPase (SERCA) 2a (red), cell membrane (green), and nuclei (blue) in embryonic day (E) 10.5, E12.5, 1-day-old neonatal, and adult mouse ventricular tissue sections. E10.5–E12.5 mouse ventricles show lower staining intensity of SERCA2a compared with older hearts. *B*, *left*: the ratio of SERCA2a fluorescence intensity to nuclear fluorescence intensity (solid bars), and the ratio of SERCA2a fluorescence intensity to membrane fluorescence intensity (shaded bars) in sections at different heart ages. *C* and *D*: the effects of thapsigargin and ryanodine (Tg+Ry at E10.5 and E11.5), isoproterenol (Iso), and verapamil (Ver) on intracellular Ca (Ca_i) transient (CaT) amplitude (*C*) and the half time ($T_{0.5}$) for CaT recovery (*D*). Values are means ± SD for the no. of hearts indicated. *$P < 0.05$.

(10). At both E10.5 and E11.5 stages, verapamil abolished Ca_i transients in all of the specimens (Fig. 1*C*).

These findings indicate that, in the embryonic mouse heart, the SR is largely nonfunctional at E10.5, but begins to contribute significantly to excitation-contraction coupling by E11.5. This is generally consistent with previous studies (12, 14, 31), indicating that the contribution of SR Ca cycling increases progressively during embryonic development.

Pacing-induced alternans under control conditions. The above observations indicate that the E10.5–E12.5 stages provide an optimal time window in which to evaluate the importance of a functional SR in the development of cardiac alternans. Figure 2*A* shows an example of simultaneous voltage and Ca_i mapping in an embryonic mouse heart at E10.5. The two atria (right and left) and two ventricles (right and left) are separated by the atrioventricular ring. Under control conditions during pacing at 2 Hz, the ventricular APD_{80} and Ca_i transient duration averaged 203 ± 27 and 322 ± 50 ms, respectively. Embryonic mouse ventricles could be paced to a CL of 146 ± 10 ms before loss of 1:1 capture. The incidence of alternans did not differ between E10.5 (60%, $n = 6/10$) vs. E11.5 or older ventricles (56%, $n = 9/16$) (Fig. 3*B*, solid bars). Overall, alternans of both APD and the Ca_i transient developed concurrently at an average pacing CL of 212 ± 34 ms, at which the DI averaged 89 ± 28 ms (Fig. 3*C*). The pacing CL at the onset of alternans also did not differ between E10.5 and E11.5 or older ventricles (230 ± 10 ms for E10.5 vs. 202 ± 39 ms for E11.5 or older, $P = 0.1$), at which the DI averaged 89 ± 33 ms for E10.5 vs. 89 ± 25 ms for E11.5 or older ($P = 0.7$) (Fig. 3*D*). During alternans, the longer APD was accompanied by the larger Ca_i transient and vice versa. The offset of alternans (the CL at which alternans resolved during the deceleration phase of the pacing protocol) was also simultaneous for APD and Ca_i, occurring at an average pacing CL of 206 ± 41 ms. Thus there was minimal hysteresis between the onset and offset of alternans (only one specimen in the control group).

The role of functional SR Ca_i cycling in alternans in embryonic mouse ventricles. We next investigated how disabling SR Ca_i cycling with Tg+Ry affected alternans. After Tg+Ry, the ventricular APD_{80} during pacing at 2 Hz decreased modestly (from 202 ± 39 to 149 ± 30 ms, $P < 0.01$). For E10.5 hearts, the incidence of alternans after Tg+Ry remained similar to control (54%, $n = 6/11$ vs. 60%, $n = 6/10$) (Fig. 3*B*). For E11.5 or older hearts, however, Tg+Ry tended to suppress alternans, but the difference did not reach statistical significance (28%, $n = 2/7$ vs. 56%, $n = 9/16$, $P = 0.2$) (Fig. 3*B*). The maximal amplitude of Ca_i alternans after Tg+Ry also did not differ significantly from control at either E10.5 (52 ± 11

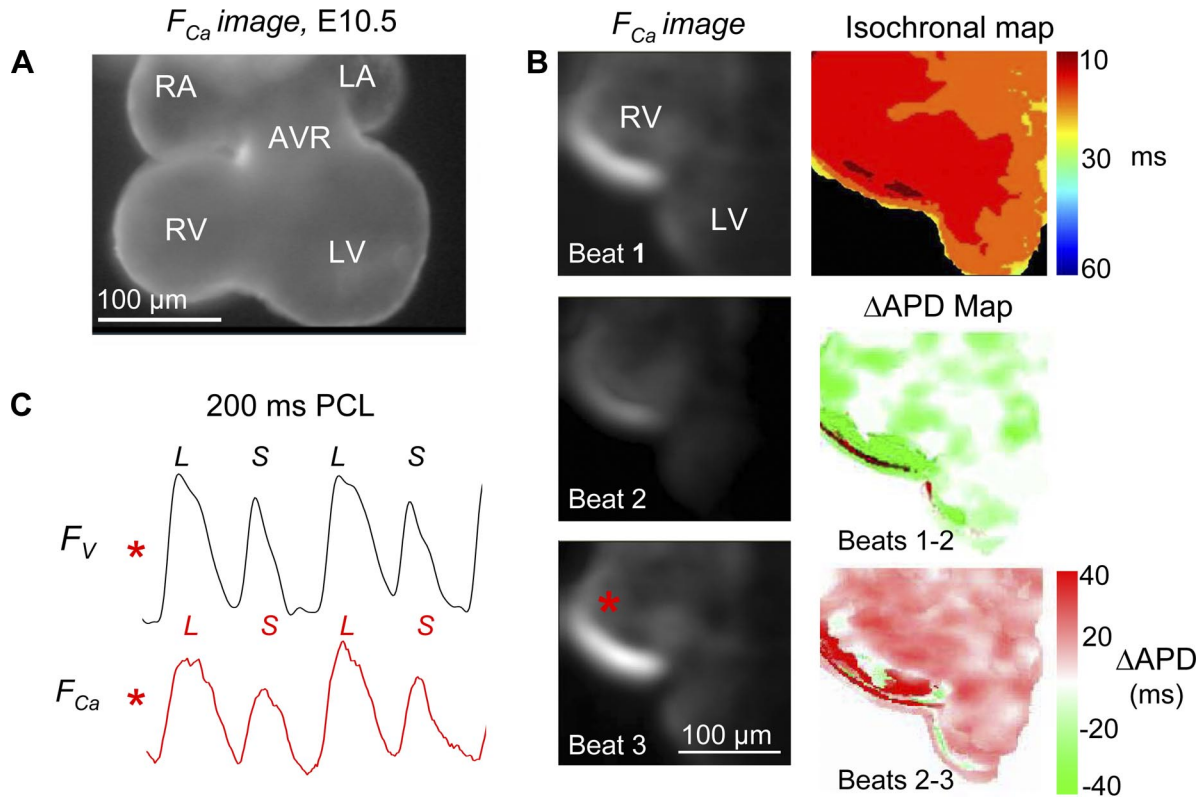

Fig. 2. Action potential duration (APD) and CaT alternans (ALT) in embryonic mouse ventricles. *A*: Ca fluorescence (F_{Ca}) image of an E10.5 mouse heart. The two atria [right (RA) and left (LA)], the atrioventricular ring (AVR), and two ventricles [right (RV) and left (LV)] are labeled. *B*: example of cardiac ALT. Consecutive F_{Ca} snapshots (*beats 1–3*) exhibited alternation in the maximum fluorescence amplitude (large-small-large). Isochronal map shows the propagation pattern across the ventricle. APD ALT maps show APD differences (Δ) between consecutive beats (*beat 1–2* and *beat 2–3*). Red and green represent positive and negative differences, respectively. *C*: traces of voltage fluorescence (F_V) and F_{Ca} at the pixel indicated by the red asterisk in *B* (*beat 3*) demonstrating CaT and APD ALT at 200-ms pacing cycle length (CL), in which the shorter APD is associated with a smaller CaT amplitude (concordant APD-Ca_i ALT). Long/large (L) and short/small (S) APD and CaT are labeled.

vs. 51 ± 10%) or E11.5–E12.5 (42 ± 6 vs. 55 ± 9%) (Fig. 3*C*). For E10.5, the average DI at the onset of alternans was similar after Tg+Ry compared with control (81 ± 27 vs. 89 ± 33 ms for the control group, Fig. 3*D*). At E11.5–E12.5, however, the average DI at the onset of alternans decreased significantly after Tg+Ry (46 ± 3 vs. 89 ± 25 ms for the control group, $P < 0.05$, Fig. 3*D*). These results indicate that, in embryonic mouse hearts, alternans occurs whether the SR is

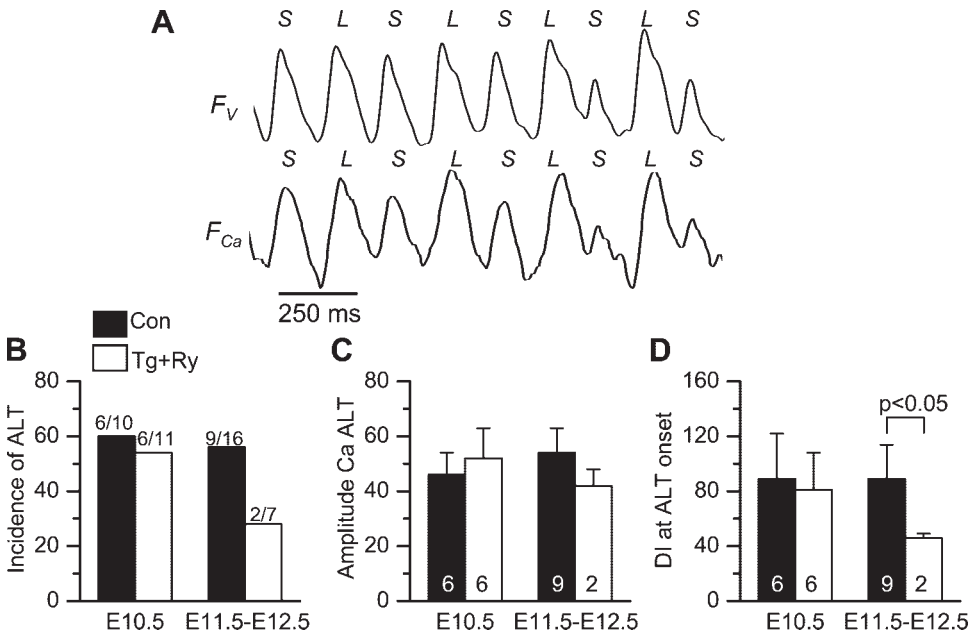

Fig. 3. Cardiac ALT in embryonic mouse ventricles after SR blockade. *A*: example of APD and CaT ALT after SR blockade with Tg+Ry at 160-ms pacing CL. L and S APD and CaT are labeled. *B–D*: the corresponding incidences, amplitude, and diastolic interval (DI) at onset of ALT before and after Tg+Ry in E10.5 vs. E11.5–E12.5 hearts. Bars indicate means ± 1 SD, for the no. of hearts indicated. $P < 0.05$ for E11.5 vs. E12.5.

essentially nonfunctional (E10.5) or significantly functional (E11.5 and older). Thus alternans in the embryo does not appear to be critically dependent on a functioning SR.

APD restitution properties and alternans in embryonic mouse hearts. If a functional SR is not essential for the development of alternans in the embryonic heart, then APD restitution slope is likely to play a key role (17). To examine how APD restitution slope correlates with the development of alternans, we compared APD restitution curves from hearts that developed alternans with those that did not (see Fig. 4*A*). As summarized in Fig. 4*B*, *left*, the maximum APD restitution slope was significantly greater in both E10.5 and E11.5–E12.5 hearts that developed alternans (open bars) than in those that did not (solid bars), averaging 2.2 ± 0.6 vs. 0.8 ± 0.4, respectively. For both age groups, the onset of alternans occurred at an average DI of 89 ± 28 ms, at which point the APD restitution slope averaged 1.3 ± 0.6 (Fig. 4*B*, *right*). In 4 of 15 hearts, however, alternans appeared when the slope of APD restitution was <1.

After Tg+Ry, the maximum APD restitution slope in hearts that developed alternans was not significantly different compared with control conditions, at either E10.5 (1.8 ± 0.4 vs. 2.3 ± 0.5 for control, $P = 0.1$) or E11.5 (1.3 ± 0.4 vs. 2.2 ± 0.6 for control, $P = 0.09$). The incidence of alternans was also not significantly different from control at either E10.5 (54 vs. 60% for control) or E11.5 (28 vs. 56% for control). In all hearts developing alternans after Tg+Ry, the maximum APD restitution slope exceeded one, averaging 1.7 ± 0.5, compared with 0.87 ± 0.6 in E10.5–E12.5 hearts without alternans ($P < 0.01$). The onset of alternans occurred at an average DI of 67 ± 28 ms, at which point the APD restitution slope was always ≥ 1 (Fig. 4*B*, *right*).

Effects of autonomic modulation on alternans and APD restitution slope in embryonic mouse hearts. Iso and CCh were used to mimic for β-receptor and muscarinic receptor stimulation, respectively. In 14 hearts studied, Iso ($n = 14$) did not significantly affect APD_{80} during pacing at 2 Hz (203 ± 27 ms after Iso vs. 214 ± 35 ms before), but Iso + CCh decreased APD_{80} significantly to 157 ± 20 ms ($P < 0.01$). Iso increased the incidence of alternans to 100% in both E10.5 and E11.5–E12.5 hearts (Fig. 5*A* and supplemental file movie 1, contained in the online version of this article). Therefore, we combined both age groups for further analysis. One-to-one capture was lost at a pacing CL of 154 ± 15 ms after Iso and 143 ± 8 ms after Iso + CCh. The onset of alternans after Iso occurred at a significantly longer pacing CL compared with control (244 ± 27 vs. 212 ± 34 ms, $P < 0.05$) and at a significantly longer DI (110 ± 23 vs. 89 ± 28, $P < 0.05$). Hysteresis between the onset and offset of alternans was uncommon (only in one specimen in the Iso group). In the presence of Iso, alternans was suppressed by the addition of CCh in six hearts (Fig. 5).

As shown in Fig. 6, *A* and *B*, Iso significantly increased the maximum APD restitution slope from 2.2 ± 0.6 ($n = 15$) to 3.6 ± 1.2 ($n = 14$, $P < 0.02$), which was reversed by subsequent addition of CCh. After Iso, the onset of alternans occurred at a significantly longer DI compared with control (108 ± 22 vs. 89 ± 28 ms, $P < 0.05$), where the slope of APD restitution averaged 1.38 ± 0.7. In 5 of 14 specimens, however, alternans occurred at a DI corresponding to an APD restitution slope < 1 (Fig. 6*C*). CCh reversed these effects (Fig. 6, *B* and *C*).

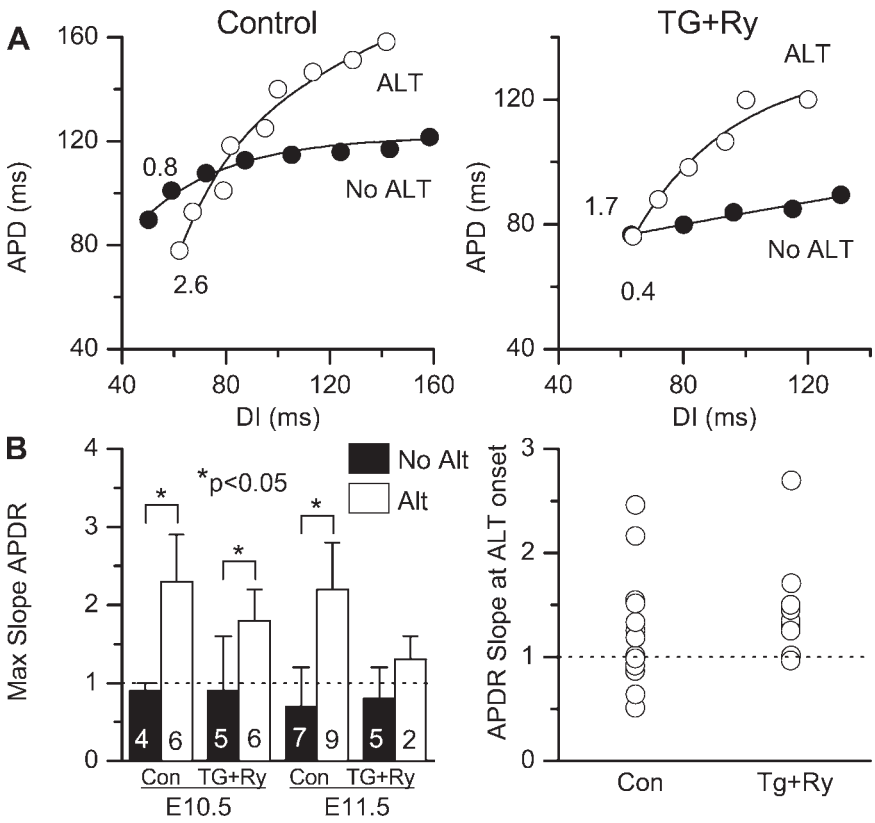

Fig. 4. APD restitution (APDR) in embryonic mouse ventricles under control conditions and after blocking SR function with Tg+Ry. *A*, *left*: representative APDR curves from two hearts: one that developed ALT (○), and one that did not (●). Nos. indicate the maximum slope of APDR obtained from monoexponential fits. *Right*: APDR curves in two hearts after Tg+Ry, one that developed ALT (○) and one that did not (●). *B*, *left*: average maximum APDR slopes in control conditions and after Tg+Ry in the hearts that developed ALT (open bars) and in those that did not (no ALT, solid bars). Dashed line indicates slope = 1. Nos. of hearts are shown. *$P < 0.05$. *Right*: for all hearts that developed ALT, the value of the APDR slope at the onset of ALT, in control conditions and after Tg+Ry.

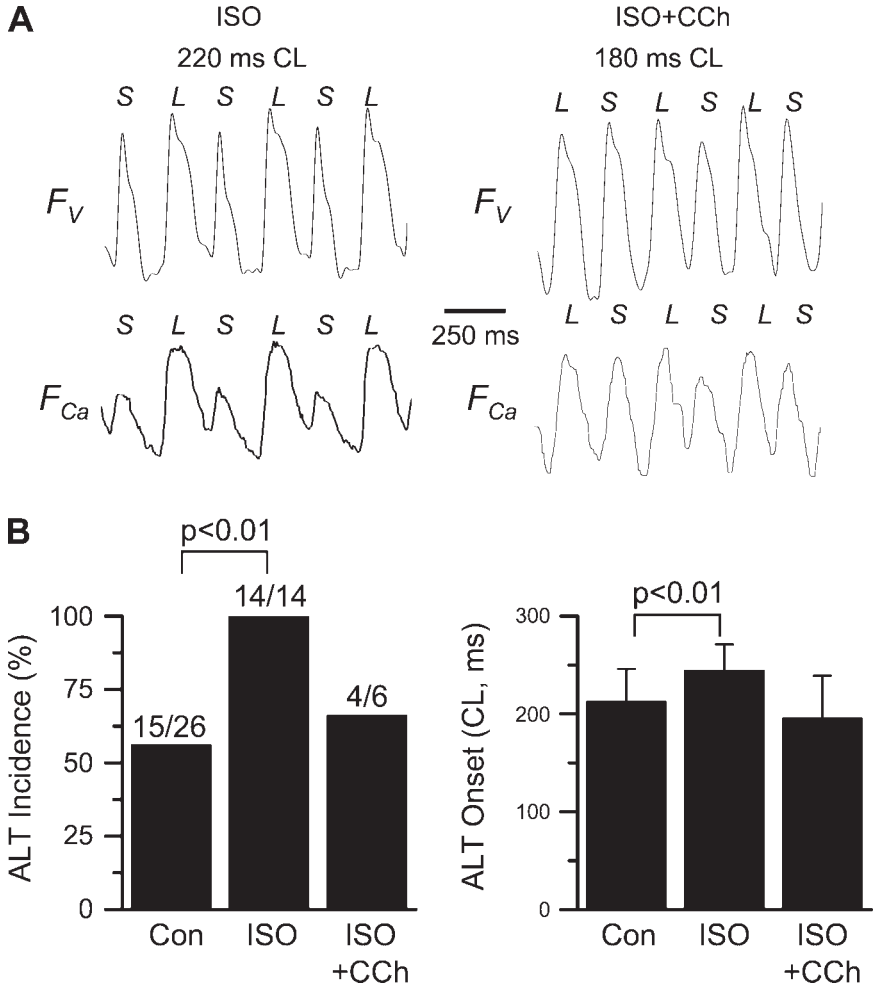

Fig. 5. Autonomic regulation of cardiac ALT in embryonic mouse ventricles. *A*: example of APD and CaT ALT during pacing at 220-ms CL in the presence of Iso. Subsequent addition of carbachol (CCh) in the same heart decreased ALT, even at 180-ms pacing CL. L and S APD and CaT are labeled. *B*: incidence of ALT and the average pacing CL at the onset of ALT under control conditions, after Iso and after Iso+CCh. No. of hearts and *P* values are indicated above the bars.

DISCUSSION

The major findings of our study are as follows: *1*) in embryonic mouse ventricles, the SR develops significant functionality between E10.5 and E11.5, a period that corresponds to 4–5 wk in human fetuses (27); *2*) both APD and Ca_i transient alternans can be induced by rapid pacing in early embryonic mouse ventricles, with a similar incidence both before and after SR Ca cycling becomes functional; *3*) alternans in embryonic ventricles generally correlates well the APD restitution slope; *4*) β-adrenergic stimulation steepens APD restitution slope and promotes alternans in embryonic mouse ventricles; and *5*) muscarinic stimulation with CCh reverses the effects of β-adrenergic stimulation on both APD restitution slope and alternans.

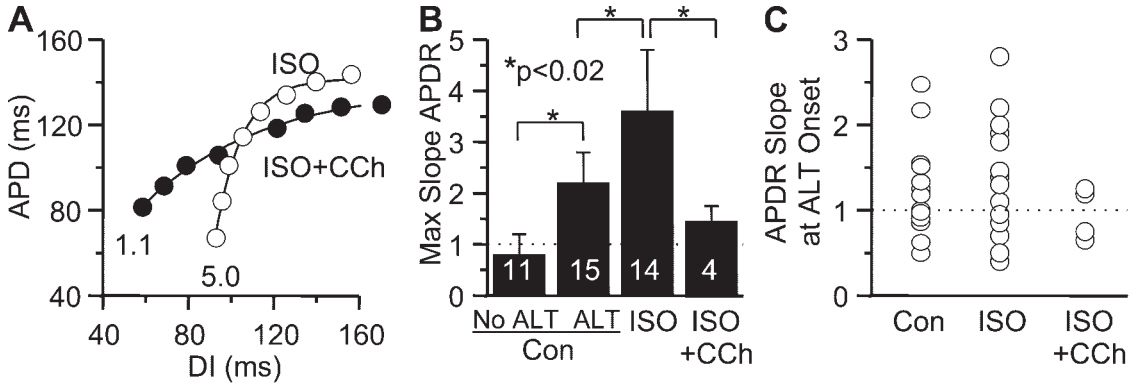

Fig. 6. Autonomic effects on APDR in embryonic mouse ventricles. *A*: APDR curves of a representative heart during Iso, (○) and after Iso+CCh (●). Nos. indicate the maximum APDR slopes obtained from the monoexponential fits. *B*: average maximum APDR slopes under control conditions, after Iso and after Iso+CCh. No. of hearts are shown. *$P < 0.02$. *C*: in all hearts that developed ALT, the distribution of APDR slopes at the onset of ALT under control conditions, after Iso and after Iso+CCh.

SR function. Previous histological and functional studies (2, 13, 15) suggest that SR Ca cycling system in mammalian hearts does not fully mature until well after birth, supporting the traditional view that transsarcolemmal Ca influx through voltage-dependent Ca channels comprises the main component of action potential-coupled Ca_i transients before birth (2). Consistent with this view, Liu et al. (12) found that SR was not functional in mouse embryonic hearts at 9.5 days postconception. However, Moorman et al. (14) found that the SR Ca cycling was functional in rat embryonic hearts at 13 days postconception. Moreover, it has also been shown that SR Ca cycling plays an important role in pacemaking activity in the embryonic hearts (31). Therefore, how quickly the SR matures and contributes to excitation-contraction coupling among different tissues in the embryonic heart remains controversial. Consistent with a minimally functional SR in embryonic mouse ventricles at E10.5, we found that SR blockade with Tg+Ry decreased the amplitude and duration of Ca_i transients by only ~10%. In contrast, the effect of Tg+Ry on the amplitude of Ca_i transient became significant (~50%) at E11.5. In addition, Tg+Ry significantly increased the half time of the Ca_i removal at E11.5, as is expected if Ca re-uptake by the SR is an important mechanism of Ca_i removal, as in adult mammalian heart (3). However, this gain of function in SR Ca cycling at E11.5 did not significantly enhance the inducibility of alternans compared with E10.5.

We have previously shown that β-adrenergic receptors are functional at these embryonic heart stages (4). At E11.5, Iso decreased the half time of the Ca_i removal, as is observed in adult heart due to Iso-mediated SERCA2a stimulation (10). L-type Ca channel inhibition with verapamil completely abolished Ca_i transients and contraction, as expected, since it eliminates transsarcolemmal Ca influx as well as the trigger for Ca-induced Ca release from the SR.

The Role of APD restitution and SR Ca_i cycling in alternans in embryonic mouse hearts. In the adult heart, the underlying mechanism of alternans was originally attributed to steep APD restitution slope (so-called voltage-driven alternans) (17). However, recent evidence (8, 11, 19) supports the idea that, in adult mammalian heart, Ca_i transient alternans, due to a dynamic instability in SR Ca cycling, also plays a key role, especially in the onset of APD alternans. However, since membrane voltage and Ca_i cycling are bidirectionally coupled, overall APD stability depends on both factors and their coupling (25, 32).

Recently, it has been reported that T-wave alternans can occur in utero in human fetuses at 14–39 wk of gestation (33). Here we found that both APD and Ca_i transient alternans can be induced by pacing at an even earlier embryonic stage in embryonic mouse ventricles, since E10.5 is equivalent to 4- to 5-wk gestation in humans. At this stage in the embryonic mouse heart, we have shown that SR Ca cycling is not yet fully functional. Thus, even if the SR is not yet functional at 14–39 wk in human fetuses, our findings suggest that APD alternans could still be explained by the APD restitution slope mechanism. Moorman et al. (14) detected SERCA2a expression at as early as 7 wk in human fetuses, but the functionality of SR Ca cycling has not been well characterized during human fetal gestation.

Under control conditions, the development of alternans correlated strongly with APD restitution slope >1, although the correlation was not perfect. For example, a minority of embryonic ventricles developed APD alternans at a DI at which APD restitution slope was still <1. This could be due to short-term memory effects, which are known to distort the relationship between the APD restitution slope >1 criteria and the onset of alternans (29). In support of a predominant role of APD restitution, when SR function was suppressed by Tg+Ry, alternans exclusively developed at APD restitution slopes > 1. Alternans occurred with similar incidence and magnitude, whether the SR Ca cycling was essentially nonfunctional (E10.5) or significantly functional (E11.5 or older), indicating that alternans is not critically dependent on a functional SR at this stage of cardiac embryogenesis. A caveat, however, is that the interaction between APD restitution slope and SR Ca_i cycling properties in producing alternans is highly interdependent (8, 23, 26), making it difficult to distinguish unequivocally their respective contributions, especially at E11.5 or older.

Autonomic effects on cardiac alternans in embryonic mouse ventricles. In the adult heart, β-adrenergic stimulation has multiple effects on membrane currents and SR Ca_i cycling. Stimulation of the L-type Ca current tends to promote alternans by steepening APD restitution slope and augmenting SR Ca loading, but enhanced SERCA activity tends to suppress alternans (32). Depending on which of these effects predominate, β-adrenergic stimulation can either promote or inhibit alternans, and both effects have been observed experimentally in mammalian ventricles (7, 16). In human ventricles, adrenergic stimulation steepens APD restitution (28), and β-blockers have been shown to flatten the APD restitution slope (8a), decrease T-wave alternans (20), and reduce sudden cardiac death in cardiomyopathy patients (1).

Our laboratory previously reported that both β-adrenergic and muscarinic receptors are present and functional in the embryonic mouse hearts at E10.5 or older (4). Consistent with a partly functional SR at this stage, we found that Iso promoted, rather than suppressed, alternans in embryonic mouse ventricles. Thus, unlike the adult heart in which β-adrenergic stimulation with Iso may often suppress alternans by enhancing Ca uptake by the SR, the major effect of Iso in embryonic mouse ventricles is to steepen APD restitution slope and thereby potentiate alternans. Muscarinic receptor stimulation by CCh in the presence of Iso reversed these effects.

Conclusions. Embryonic mouse ventricles without significantly functional SR Ca cycling can develop cardiac alternans, which is generally well correlated to APD restitution slope and is modulated by autonomic factors.

ACKNOWLEDGMENTS

This study was supported by Grants from the American Heart Association (0625048Y to C. de Diego; 0365133Y and 0565149Y to M. Valderrábano), the National Heart, Lung, and Blood Institute (P50 HL52319 and P01 HL078931 to J. N. Weiss), and the Laubisch and Kawata Endowments (to J. N. Weiss).

GRANTS

We thank Lingqin Pan for excellent technical assistance.

REFERENCES

1. **[Anon].** The Cardiac Insufficiency Bisoprolol Study II (CIBIS-II): a randomised trial. *Lancet* 353: 9–13, 1999.
2. **Arai M, Otsu K, MacLennan DH, Periasamy M.** Regulation of sarcoplasmic reticulum gene expression during cardiac and skeletal muscle development. *Am J Physiol Cell Physiol* 262: C614–C620, 1992.

3. **Bassani RA, Bassani JW, Bers DM.** Mitochondrial and sarcolemmal Ca^{2+} transport reduce $[Ca^{2+}]_i$ during caffeine contractures in rabbit cardiac myocytes. *J Physiol* 453: 591–608, 1992.
4. **Chen F, Klitzner TS, Weiss JN.** Autonomic regulation of calcium cycling in developing embryonic mouse hearts. *Cell Calcium* 39: 375–385, 2006.
5. **Chudin E, Goldhaber J, Garfinkel A, Weiss J, Kogan B.** Intracellular Ca(2+) dynamics and the stability of ventricular tachycardia. *Biophys J* 77: 2930–2941, 1999.
6. **Diaz ME, Eisner DA, O'Neill SC.** Depressed ryanodine receptor activity increases variability and duration of the systolic Ca^{2+} transient in rat ventricular myocytes. *Circ Res* 91: 585–593, 2002.
7. **Euler DE, Guo H, Olshansky B.** Sympathetic influences on electrical and mechanical alternans in the canine heart. *Cardiovasc Res* 32: 854–860, 1996.
8. **Goldhaber JI, Xie LH, Duong T, Motter C, Khuu K, Weiss JN.** Action potential duration restitution and alternans in rabbit ventricular myocytes: the key role of intracellular calcium cycling. *Circ Res* 96: 459–466, 2005.

8a. **Hao SC, Christini DJ, Stein KM, Jordan PN, Iwai S, Bramwell O, Markowitz SM, Mittal S, Lerman BB.** Effect of β adreneigic blockade on dynamic electrical restitution in vivo. *Am J Physiol Heart Circ Physiol* 287: H390–H394, 2004.

9. **Karma A.** Electrical alternans and spiral wave breakup in cardiac tissue. *Chaos* 4: 461–472, 1994.
10. **Kavaler F, Morad M.** Paradoxical effects of epinephrine on excitation-contraction coupling in cardiac muscle. *Circ Res* 18: 492–501, 1966.
11. **Laurita KR, Katra R, Wible B, Wan XP, Koo MH.** Transmural heterogeneity of calcium handling in canine. *Circ Res* 92: 668–675, 2003.
12. **Liu W, Yasui K, Opthof T, Ishiki R, Lee JK, Kamiya K, Yokota M, Kodama I.** Developmental changes of Ca(2+) handling in mouse ventricular cells from early embryo to adulthood. *Life Sci* 71: 1279–1292, 2002.
13. **Lompre AM, Lambert F, Lakatta EG, Schwartz K.** Expression of sarcoplasmic reticulum Ca(2+)-ATPase and calsequestrin genes in rat heart during ontogenic development and aging. *Circ Res* 69: 1380–1388, 1991.
14. **Moorman AF, Schumacher CA, de Boer PA, Hagoort J, Bezstarosti K, van den Hoff MJ, Wagenaar GT, Lamers JM, Wuytack F, Christoffels VM, Fiolet JW.** Presence of functional sarcoplasmic reticulum in the developing heart and its confinement to chamber myocardium. *Dev Biol* 223: 279–290, 2000.
15. **Nakanishi T, Okuda H, Kamata K, Abe K, Sekiguchi M, Takao A.** Development of myocardial contractile system in the fetal rabbit. *Pediatr Res* 22: 201–207, 1987.
16. **Nearing BD, Huang AH, Verrier RL.** Dynamic tracking of cardiac vulnerability by complex demodulation of the T wave. *Science* 252: 437–440, 1991.
17. **Nolasco JB, Dahlen RW.** A graphic method for the study of alternation in cardiac action potentials. *J Appl Physiol* 25: 191–196, 1968.
18. **Pastore JM, Girouard SD, Laurita KR, Akar FG, Rosenbaum DS.** Mechanism linking T-wave alternans to the genesis of cardiac fibrillation. *Circulation* 99: 1385–1394, 1999.
19. **Pruvot EJ, Katra RP, Rosenbaum DS, Laurita KR.** Role of calcium cycling versus restitution in the mechanism of repolarization alternans. *Circ Res* 94: 1083–1090, 2004.
20. **Rashba EJ, Cooklin M, MacMurdy K, Kavesh N, Kirk M, Sarang S, Peters RW, Shorofsky SR, Gold MR.** Effects of selective autonomic blockade on T-wave alternans in humans. *Circulation* 105: 837–842, 2002.
21. **Reuter H, Henderson SA, Han T, Mottino GA, Frank JS, Ross RS, Goldhaber JI, Philipson KD.** Cardiac excitation-contraction coupling in the absence of Na^+-Ca^{2+} exchange. *Cell Calcium* 34: 19–26, 2003.
22. **Rosenbaum DS, Jackson LE, Smith JM, Garan H, Ruskin JN, Cohen RJ.** Electrical alternans and vulnerability to ventricular arrhythmias. *N Engl J Med* 330: 235–241, 1994.
23. **Sato D, Shiferaw Y, Garfinkel A, Weiss JN, Qu Z, Karma A.** Spatially discordant alternans in cardiac tissue: role of calcium cycling. *Circ Res* 99: 520–527, 2006.
25. **Shiferaw Y, Sato D, Karma A.** Coupled dynamics of voltage and calcium in paced cardiac cells. *Phys Rev E Stat Nonlin Soft Matter Phys* 71: 021903, 2005.
26. **Shiferaw Y, Watanabe MA, Garfinkel A, Weiss JN, Karma A.** Model of intracellular calcium cycling in ventricular myocytes. *Biophys J* 85: 3666–3686, 2003.
27. **Sissman NJ.** Developmental landmarks in cardiac morphogenesis: comparative chronology. *Am J Cardiol* 25: 141–148, 1970.
28. **Taggart P, Sutton P, Chalabi Z, Boyett MR, Simon R, Elliott D, Gill JS.** Effect of adrenergic stimulation on action potential duration restitution in humans. *Circulation* 107: 285–289, 2003.
29. **Tolkacheva EG, Schaeffer DG, Gauthier DJ, Krassowska W.** Condition for alternans and stability of the 1:1 response pattern in a "memory" model of paced cardiac dynamics. *Phys Rev E Stat Nonlin Soft Matter Phys* 67: 031904, 2003.
30. **Valderrabano M, Chen F, Dave AS, Lamp ST, Klitzner TS, Weiss JN.** Atrioventricular ring reentry in embryonic mouse hearts. *Circulation* 114: 543–549, 2006.
31. **Viatchenko-Karpinski S, Fleischmann BK, Liu Q, Sauer H, Gryshchenko O, Ji GJ, Hescheler J.** Intracellular Ca^{2+} oscillations drive spontaneous contractions in cardiomyocytes during early development. *Proc Natl Acad Sci USA* 96: 8259–8264, 1999.
32. **Weiss JN, Karma A, Shiferaw Y, Chen PS, Garfinkel A, Qu Z.** From pulsus to pulseless: the saga of cardiac alternans. *Circ Res* 98: 1244–1253, 2006.
33. **Zhao H, Strasburger JF, Cuneo BF, Wakai RT.** Fetal cardiac repolarization abnormalities. *Am J Cardiol* 98: 491–496, 2006.